Supporting information

Efficient and effective removal of toluene from aqueous solution using MIL-100(Fe)

Catalina V. Flores,[a,b] Juan L. Obeso, [a,b] Herlys Viltres,[c] Ricardo A. Peralta,[d*] Ilich A. Ibarra[b,e*] and Carolina Leyva[a*]

[a]*Instituto Politécnico Nacional, CICATA U. Legaria, Laboratorio Nacional de Ciencia, Tecnología y Gestión Integrada del Agua (LNAgua), Legaria 694, Col. Irrigación, Miguel Hidalgo, 11500, CDMX, México.*

[b]*Laboratorio de Fisicoquímica y Reactividad de Superficies (LaFReS), Instituto de Investigaciones en Materiales, Universidad Nacional Autónoma de México, Circuito Exterior s/n, CU, Coyoacán, 04510, Ciudad de México, México.*

[c]*School of Engineering Practice and Technology, McMaster University, 1280 Main Street West Hamilton, ON, L8S 4L8, Canada.*

[d]*Departamento de Química, División de Ciencias Básicas e Ingeniería. Universidad Autónoma Metropolitana (UAM-I), 09340, México.*

[e]*On sabbatical as "Catedra Dr. Douglas Hugh Everett" at Departamento de Química, Universidad Autónoma Metropolitana-Iztapalapa, Avenida San Rafael Atlixco 186, Leyes de Reforma 1ra Sección, Iztapalapa, 09310 Ciudad de México, México*

Section S1: Analytical instruments

X-ray diffraction (XRD) analysis was performed using a D5000 type equipment, Siemens, Germany. Cu radiation was used. The analyzed range of diffraction angle 2θ was between 3 and 50° with a step width of 0.028°. Fourier-transform infrared spectroscopy (FT-IR) spectra were obtained in the 4000-400 cm^{-1} range on a Shimadzu IRTracer-100 spectrometer using KBr pellets. Thermal gravimetric analysis (TGA) was performed using a TA Instruments Q500HR analyzer under an N_2 atmosphere using the high-resolution mode (dynamic rate TGA) at a 2 °C min^{-1} scan rate from room temperature to 800 °C. The zeta potentials were measured using NanoPlus HD sizer equipment (Micrometrics, USA). Zeta potential values were measured in a 2-10 pH range. A minimum of 3 measurements per sample was done at room temperature. The pH variation was carried out using 0.01 M NaOH and HNO_3 solutions. X-ray photoelectron Spectroscopy (XPS) analyses were carried out with a Thermo Scientific K-alpha X-ray photoelectron spectrometer working at 72 W and equipped with a hemispherical analyzer and a monochromatic. Survey scans were recorded using 400 μm spot size and fixed pass energy of 200 eV, whereas high-resolution scans were collected at 20 eV of pass energy. Spectra have been charged and corrected to the mainline of the carbon 1s spectrum (adventitious carbon) set to 284.8 eV. Spectra were analyzed using CasaXPS software (version 2.3.14). Spectral backgrounds were subtracted using the Shirley method. Curve fitting procedures and elemental quantifications were performed with the CasaXPS program (version 2.3.14). The pH measurements were made using the Acorn® pH 5 Meter (OAKTON, USA). The morphology was analyzed employing a variable pressure scanning electron microscope (SEM), brand FEI Co. and Quanta model FEG 250 with an EDS detector Bruker model XFlash 6160. Nitrogen adsorption-desorption isotherms were measured by a volumetric method using a Micromeritics ASAP 2020 gas sorption analyzer. The sample mass was

65.0 mg. Free space correction measurements were performed using ultra-high purity He gas (UHP grade 5, 99.999% pure). Nitrogen isotherms were measured using UHP grade Nitrogen. All nitrogen analyses were performed using a liquid nitrogen bath at 77 K. Oil-free vacuum pumps were used to prevent contamination of sample or feed gases. The residual toluene determination was through the PerkinElmer gas chromatograph, model Claurus 480, coupled with the flame ionization detector (FID), using the Elite-1 (30 m x 0.32 mm I.D. x 0.25 µm) column, employing nitrogen as carrier gas.

Section S2: Experimental

1. **Synthesis of MIL-100(Fe)**

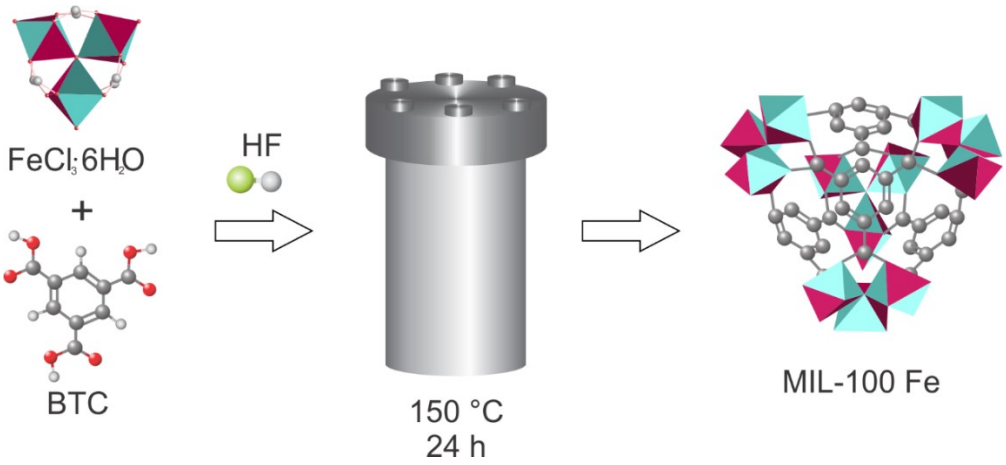

Figure S1. MIL-100(Fe) synthesis schematic.

2. **Adsorption experiments**

Experiments were carried out in triplicate. Toluene adsorption evaluations were performed by adding a MIL-100(Fe) mass (1-30 mg) in a fixed volume (20 mL) with a toluene initial concentration (5-150 mg L^{-1}) under stirring for 24 h, under controlled pH (2-10). Through gas chromatography coupled to a flame ionization detector, the residual amount of toluene was analysed using liquid-liquid extraction.

a) Adsorbent dosage influence

The effect of the mass adsorbent mass over the toluene adsorption was evaluated by adding 1, 5, 10, 20, and 30 mg of MIL-100(Fe) to 20 mL solution with 100 mg L^{-1} of toluene under stirring for 1440 min.

b) Solution pH influence

To study the effect of solution pH, adsorption experiments were carried out at pH 2, 4, 6, 8, and 10 by adding 10 mg of MIL-100(Fe) to 20 mL (100 mg L^{-1}) of the toluene solution, under stirring for 1440 min. The pH values were adjusted using 0.1 mol L^{-1} HNO_3/NaOH.

c) Contact time influence

To evaluate the effect of contact time, 10 mg of MIL-100(Fe) were placed in 20 mL with 100 mg L^{-1} of toluene under stirring. Separate experiments were performed for each period, 3, 5, 15, 30, 30, 60, 60, 120, 180, 480, and 1440 min.

d) Initial concentration influence

The variation of initial concentration of toluene was valued at 5, 10, 20, 30, 40, 50, 60, 70, 80, 100, 110, 120, 130, 140, and 150 mg L^{-1}. 10 mg of MIL-100(Fe) were added to 20 mL of toluene solution under stirring for 1440 min.

e) Regeneration experiments

The regeneration effect was evaluated by five cycles with 20 mL of toluene solution 100 mg L^{-1} of concentration with 10 mg of MIL-100(Fe) under stirring for 1440 min. For desorption, the exhausted MIL-100(Fe) was placed inside a fume hood at 110 °C for 8 hours for each desorption step.

f) Interferents VOCs influence

To evaluate the adsorption of toluene in the presence of other VOCs, the adsorption was evaluated in the presence of benzene, xylene, and a mixture of the three VOCs: toluene, benzene, and xylene. For this purpose, 10 mg of MOFs were placed in 20 mL of a solution containing 100 mg L^{-1} of toluene and benzene, a second solution containing 100 mg L^{-1} of toluene and xylene, and a third solution containing 100 mg L^{-1} of toluene, benzene, and xylene, under agitation for 1440 min.

g) Kinetic adsorption experiments

The kinetic models evaluated were the pseudo-first-order (PFO), pseudo-second-order (PSO), Elovich, and Intra-particle diffusion (IPD) using the non-linear equations in the experimental adsorption capacity data. The equations employed are summarized in Table S6.

h) Adsorption isotherms experiments

Adsorption isotherms were analyzed to determine the possible interaction of toluene molecules with the surface of MOFs within the liquid phase. The non-linear fitting of the Langmuir, Freundlich, and Temkin models was performed. The non-linear equations are summarized in Table S8.

3. Toluene quantification

a) Sample extraction

The method employed was similar to Yusiasih and collaborators.[2] The aqueous sample was added to a separation funnel with the organic phase, n-hexane; it was shaken and allowed to settle until the phases were separated. The aqueous phase was extracted a second time. In a separation funnel, the extracted organic phase, n-hexane, was placed with saturated anhydrous magnesium sulfate to dry the organic phase. The funnel was shaken and allowed to stand to separate the phases. The n-

hexane was preconcentrated in a water bath at 60 °C. The preconcentrate is transferred to a volumetric flask with the internal standard of chlorobenzene at a fixed concentration, and finally, it is diluted with n-hexane.

b) Chromatographic method conditions

The detection and quantification of toluene by GC-FID were done under the following conditions: The injector and detector temperatures were 200 and 250 °C, respectively. The oven temperature was varied in two stages. The first stage was at 50 °C held for 2 min, followed by an increase up to 100 °C at a rate of 20 °C min^{-1}. The injected sample was 0.5 µL. Nitrogen was the carrier gas employed.

c) Residual toluene determination

The equilibrium adsorption capacity (mg g^{-1}), Q_e, of toluene was calculated according to equation (1):

$$Q_e = \frac{(C_0 - C_e)V}{M} \quad (1)$$

Where C_0 and C_e (mg L^{-1}) are the initial and equilibrium concentration of toluene, V is the volume solution (L), and M is the dried mass adsorbent added (g).

The *removal efficiency* (%) of toluene adsorption was calculated according to equation (2):

$$Removal\ efficeiency = \left(\frac{(C_0 - C_e)}{C_0}\right)100 \quad (2)$$

Section S3: MIL-101(Fe) characterization

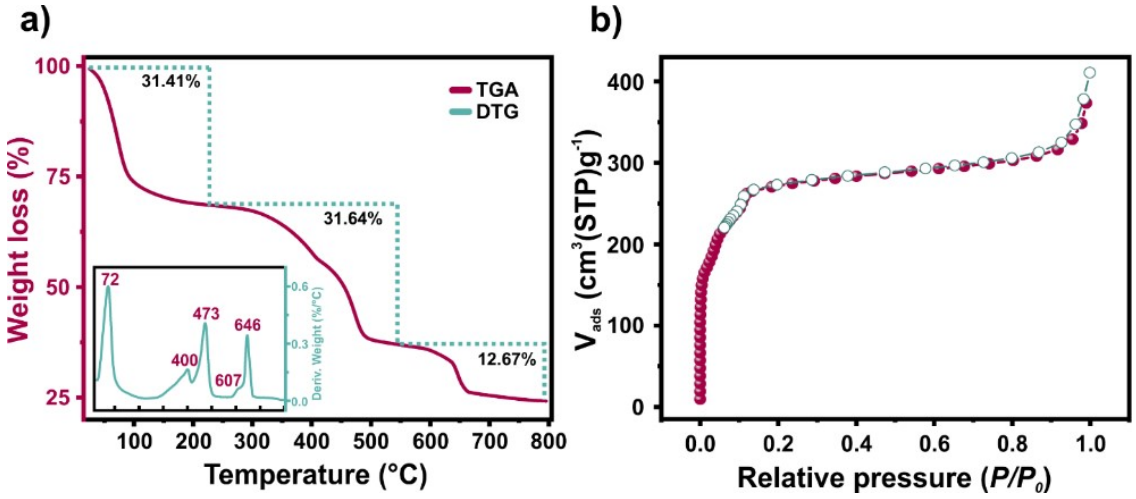

Figure S2. a) TGA-DTG analysis, and b) nitrogen adsorption isotherm of MIL-100(Fe).

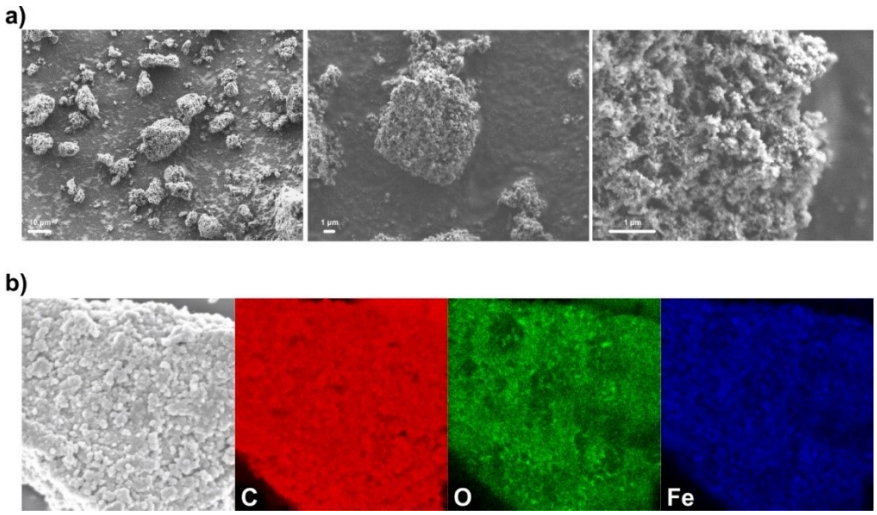

Figure S3. a) SEM micrographs of 1 000, 5 000, and 20 000 amplifications, and b) elemental mapping of MIL-100(Fe) before toluene adsorption at 5 000 amplifications.

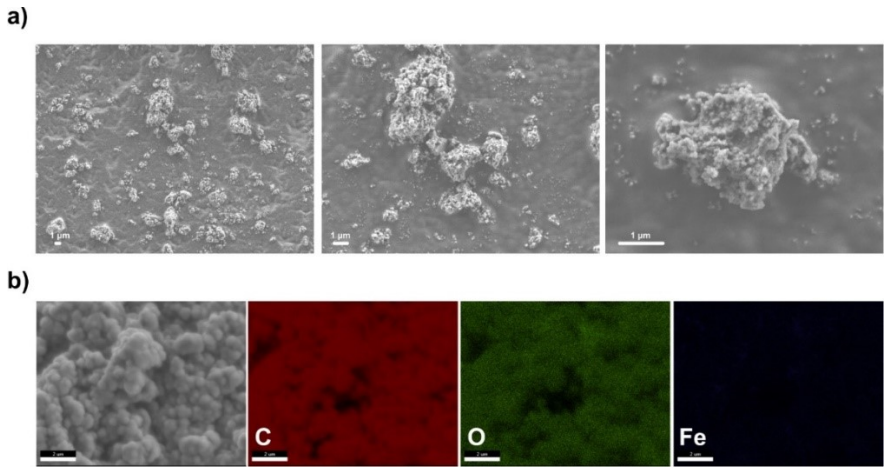

Figure S4. a) SEM micrographs of 3 000, 7 000, and 20 000 amplifications, and b) elemental mapping of MIL-100(Fe) after toluene adsorption at 10 000 amplifications.

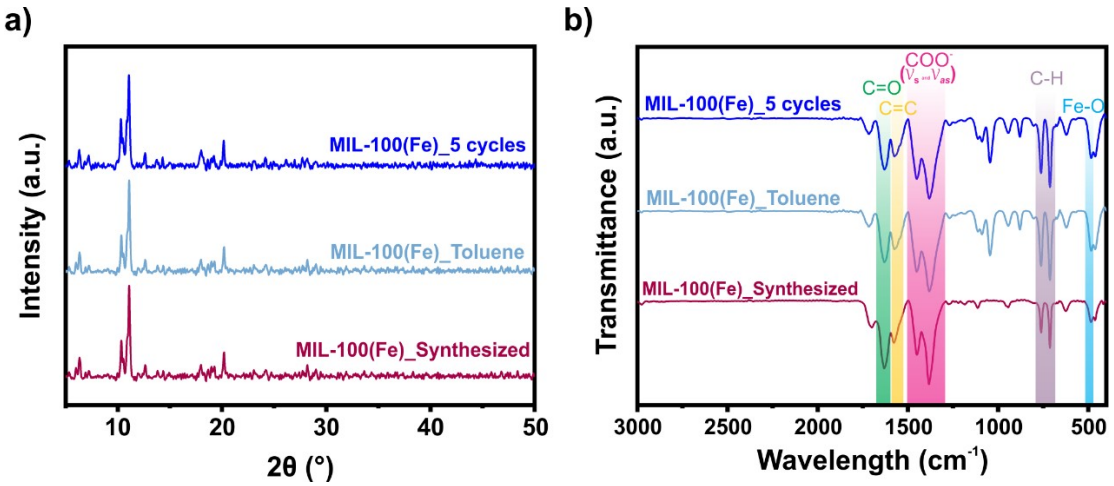

Figure S5. a) PXRD patterns and b) FT-IR spectra of MIL-100(Fe) as-synthetized, after toluene adsorption, and adsorption-desorption toluene cycles.

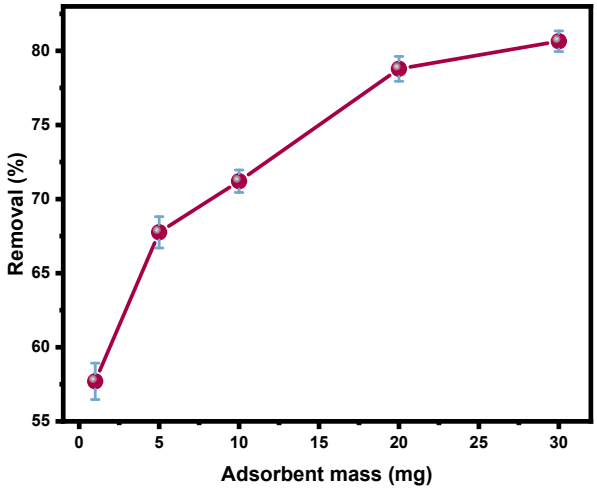

Figure S6. Adsorbent mass effect in toluene adsorption using MIL-100(Fe).

Table S1. XPS survey data (atomic percentage) of the different elements in the materials.

Samples	**Elements (At. %)**		
	C 1s	**O 1s**	**Fe 2p**
Mil-100-Fe	66.4	28.6	4.9
Mil-100-Fe + T	68.6	27.3	4.2

Table S2. The peak-fitting results of C 1s high-resolution signal of MIL-100 Fe.

Samples	**Assignment**	**E_B (eV)**	**FWHM (eV)**	**At. %**
Mil-100-Fe	**C1s** $_{C=C\ aromatic}$	284.1	1.3	18.1
	C1s $_{C-C/C-H}$	285.0	1.4	52.3
	C1s $_{C-O,\ C-O-C}$	286.1	1.5	8.4
	C1s $_{OH-C=O}$	288.9	1.7	21.2

Mil-100-Fe + T	**C1s** $_{C=C\ aromatic}$	284.1	1.3	15.1
	C1s $_{C-C/C-H}$	285.0	1.4	54.4
	C1s $_{C-O,\ C-O-C}$	286.1	1.5	10.9
	C1s $_{OH-C=O}$	288.9	1.7	19.6

Table S3. The peak-fitting results of O 1s high-resolution signal of MIL-100 Fe.

Samples	**Assignment**	**E_B (eV)**	**FWHM (eV)**	**At. %**
Mil-100-Fe	**O1s** $_{Fe-O}$	529.8	1.4	20.1
	O1s $_{O-C=O}$	530.9	1.5	65.0
	O1s $_{O\_Chemisorbed}$	532.3	1.7	14.7
Mil-100-Fe + T	**O1s** $_{Fe-O}$	529.7	1.4	18.0
	O1s $_{O\_Lattice}$	530.8	1.5	63.7
	O1s $_{O\_Chemisorbed}$	532.2	1.7	18.3

Table S4. The peak-fitting results of Fe $2p_{3/2}$ high-resolution signal of MIL-100 Fe.

Sample	**Assignment**	***E_B* (eV)**	**FWHM (eV)**	**At. %**
Mil-100-Fe	Fe^{2+}	709.2	1.7	12.0
	Fe^{3+}	711.0	1.8	33.4
	Fe^{3+}	712.2	1.9	29.1
	Fe^{3+}	713.6	2.5	25.4
	Satellite Fe^{3+}	717.0	3.9	-
Mil-100-Fe + T	Fe^{2+}	709.0	1.7	10.4
	Fe^{3+}	710.7	1.8	31.7
	Fe^{3+}	711.7	1.8	26.1

	Fe^{3+}	713.1	2.5	31.8
	Satellite Fe^{3+}	716.8	3.8	-

Section S4: Kinetics models, isotherms models, data modelling.

Table S5. Langmuir Adsorption capacity of toluene using reported MOF-based adsorbents and conventional materials.

Adsorbent	**Experimental conditions**			q_e	**Ref**
	pH	**Dosage ($g\ L^{-1}$)**	**Time (h)**	**($mg\ g^{-1}$)**	
Ni-Zeolite 4A	10	50	1.25	0.9	3
Activated carbon	5.4	0.4	0.5	263.16	4
Carbon nanotubes	6	0.25	9	105	5
Actived carbon/lignin	7	5	12	118.4	6
Hydrogel GEL-SBA15	7	0.4	3	596.6	7
Resin	5.86	5	6	78.9	8
Ostrich bone waste	7	10	6	328	9
UiO-66	-	0.5	1	22.5	10
MIL-100(Fe)	6	0.5	24	318.48	**This Work**

Table S6. Kinetic model equations and parameters.

Model	Non-linear equation	Parameters
Pseudo-first-order	$Q_t = Q_e\left(1 - e^{-k_1 t}\right)$	Q_e: adsorption capacities at equilibrium ($mg\ g^{-1}$); Q_t: adsorption capacities at a time ($mg\ g^{-1}$); k_1: pseudo-first-order rate

		constant for the kinetic model (mg g^{-1} min^{-1}); t: time (min)
Pseudo-second-order	$Q_t = \frac{k_2 Q_e^2 t}{1 + k_2 Q_e t}$ $h = k_2 \times {Q_e}^2$	Q_t: adsorption capacities at time t (mg g^{-1}); Q_e: adsorption capacities at equilibrium (mg g^{-1}); k_2: pseudo-second-order rate constant of adsorption (mg g^{-1} min^{-1}); h: initial adsorption rate (mg g^{-1} min^{-1})
Elovich	$Q_t = \frac{1}{\beta}\ln(1 + \alpha\beta t)$	Q_t: adsorption capacities at time t (mg g^{-1}); α: adsorption equilibrium constant (mg g^{-1} min^{-1}); β: equilibrium constant desorption (g mg^{-1})
Intraparticle diffusion	$Q_t = K_{id} t^{0.5} + C_i$	Q_t: adsorption capacities at time t (mg g^{-1}); K_{id}: rate parameter of stage i (mg g^{-1} $min^{-1/2}$); C_i: intercept of stage i that gives an idea about of the thickness of boundary layer (mg g^{-1}).

Table S7. Parameters of the kinetic models.

Model	Parameter	MIL-100 Fe
PFO model	q_e *(mg g^{-1})*	137.32
	K_1 *(mg g^{-1} min^{-1})*	0.025
	R^2	0.657
PSO model	q_e *(mg g^{-1})*	146.74
	K_2 *(mg g^{-1} min^{-1})*	2.88E-4
	h	6.21
	R^2	0.792
Elovich model	*β (mg g^{-1})*	0.048
	α (mg g^{-1} min^{-1})	35.61
	R^2	0.950
IPD model	K_{ip} *(mg g^{-1} min^{-1})*	3.288
	C_i *(mg g^{-1})*	57.613
	R^2	0.843

Table S8. Adsorption isotherm equation and parameters.

Model	Non-linear equation	Parameters

Langmuir	$Q_e = \frac{Q_m \times K_L \times C_e}{1 + K_L \times C_e}$ $R_L = \frac{1}{1 + K_L \times C_o}$ $\Delta G = -RTln(K_O)$ $Ko = K_L \times MM \times 10^3$	Q_m: is maximum adsorption capacity (mg g^{-1}); Q_e: the amount of adsorbate in the adsorbent at equilibrium (mg g^{-1}); K_L: is adsorption intensity or Langmuir coefficient (L mg^{-1}); C_e: is the concentration of absorbate at equilibrium (mg L^{-1}); R_L: is separation factor; ΔG: free Gibbs energy (kJ mol^{-1}); T: temperature (K); R: molar gas constant (J K^{-1} mol^{-1}); MM: Molar mass (g mol^{-1})
Freundlich	$Q_e = K_F \times C_e{}^{1/n}$	K_F: is the constant indicative of the relative adsorption capacity (L g^{-1}); n: is indicative of the intensity
Temkin	$Q_e = \frac{RT}{b_t} ln(A_t \times Ce)$ $B = \frac{RT}{b_t}$	A_t: Temkin isotherm equilibrium binding constant (L g^{-1}); b_t: Temkin isotherm constant; B: Constant related to the heat of sorption (J mol^{-1})

Table S9. Parameters of the isotherm's models.

Model	Parameter	MIL-100(Fe)
Freundlich	K_F *(L g^{-1})*	30.16
	n	1.81
	χ^2	407.71
	R^2	0.937
Langmuir	Q_m *(mg g^{-1})*	318.48
	K_L *(L mg^{-1})*	0.058
	R_L	0.773 - 0.145
	ΔG(kJ mol^{-1})	-21.29
	χ^2	240.20
	R^2	0.963
Temkin	A_t *(L g^{-1})*	0.559
	b_t	34.47
	B (J mol^{-1})	0.071
	χ^2	104.08
	R^2	0.982

References

1 X.-Z. Guo, S.-S. Han, J.-M. Yang, X.-M. Wang, S.-S. Chen and S. Quan, *Ind. Eng. Chem. Res.*, 2020, **59**, 2113–2122.
2 R. Yusiasih, R. Marvalosha, S. D. S. Suci, E. Yuliani and M. M. Pitoi, *IOP Conf. Ser.: Earth Environ. Sci.*, 2019, **277**, 012019.
3 Z. Mamaghanifar, A. Heydarinasab, A. Ghadi and E. Binaeian, *Water Conserv Sci Eng*, 2020, **5**, 1–13.
4 H. Anjum, K. Johari, N. Gnanasundaram, A. Appusamy and M. Thanabalan, *Journal of Molecular Liquids*, 2019, **280**, 238–251.
5 B. A. Abussaud, *Sustainability*, 2021, **13**, 11716.
6 M. A. Abdel-Aziz, S. A. Younis, Y. M. Moustafa and M. M. H. Khalil, *Journal of Environmental Management*, 2019, **233**, 459–470.
7 J. S. Da Costa, E. G. Bertizzolo, D. Bianchini and A. R. Fajardo, *Journal of Hazardous Materials*, 2021, **418**, 126405.
8 T. P. Makhathini and S. Rathilal, *South African Journal of Chemical Engineering*, 2017, **23**, 71–80.
9 M. Arshadi, H. Shakeri and J. W. L. Salvacion, *RSC Adv.*, 2016, **6**, 14290–14305.
10 R. Navarro Amador, L. Cirre, M. Carboni and D. Meyer, *Journal of Environmental Management*, 2018, **214**, 17–22.